Pilot-scale assessment of the viability of UVA radiation for H2O2 or S2O82– activation in advanced oxidation processes

Anaëlle Gabet, Christine de Brauer, Gilles Mailhot, Marcello Brigante, Hélène Métivier

Pilot-scale assessment of the viability of UVA radiation for H_2O_2 or $S_2O_8^{2-}$ activation in advanced oxidation processes

Anaëlle Gabet[1,2], Christine de Brauer[1], Gilles Mailhot[2], Marcello Brigante[2], Hélène Métivier[1,*1]

[1] Univ Lyon, INSA Lyon, DEEP, EA7429, 69621 Villeurbanne, France

[2] Université Clermont Auvergne, CNRS, Clermont Auvergne INP, Institut de Chimie de Clermont-Ferrand, F-63000 Clermont-Ferrand, France

Abstract

UVA and UVC radiation were compared for the activation of H_2O_2 or $S_2O_8^{2-}$ to remove micropollutants remaining in treated wastewater with a view to optimising the cost and/or the efficiency of the commonly studied UVC/H_2O_2 process. Experiments were carried out in a dynamic laboratory pilot (20 L). In a simple matrix, UVA radiation were able to produce oxydative radicals from H_2O_2 or $S_2O_8^{2-}$, although faster degradation of the estrogens was observed under UVC radiation (up to 55-fold). With both UV radiation, $S_2O_8^{2-}$ was photolyzed faster than H_2O_2, resulting in faster estrogen degradation (up to 12-fold). Coupling UVA to H_2O_2 was considered not to be viable because less than 4% of the compounds were degraded at 1000 mJ cm^{-2}. In a treated wastewater, estrogen degradations were inhibited due to organic matter and stronger inhibitions were observed with $S_2O_8^{2-}$ processes (up to 80% inhibition compared to simple matrix). The UVC/$S_2O_8^{2-}$-process still achieved the fastest degradation rate, but is roughly comparable to the UVC/H_2O_2-process. Very low degradation rates obtained with UVA/$S_2O_8^{2-}$ limit the interest in the process. Experiments were also carried out on a mixture of pharmaceuticals leading to similar conclusions.

* corresponding author. Tel:+33-472-436-288. E-mail: helene.metivier@insa-lyon.fr

Keywords: AOPs, micropollutants, photolysis, pilot scale, UVA radiation, wastewater.

1. Introduction

Water scarcity is about to be one of the major challenges of the next decades. The European Union Water Framework Directive adopted in 2000 aims at protecting the quality and the quantity of water bodies in the European Union. Although significant improvements were observed within the last decades regarding the quality of water bodies, the presence of anthropogenic micropollutants in surface and ground waters is increasingly reported. Wastewater treatment plants (WWTPs), whether they are conventional or wetlands, are one of the major gateways of micropollutants to the environment because a large panel of compounds is refractory to the treatments that are commonly used. As a consequence, effluents are released to the environment with micropollutants at concentrations up to several tens of $\mu g\ L^{-1}$ [1, 2, 3]. Improving the removal of micropollutants in WWTPs by the use of appropriate treatments would allow the discharge of water of better quality. Moreover, it could promote effluent reuse for crop fields irrigation or industrial use for example and decrease the pressure on aquatic environments.

In France, more than 90% of the WWTPs are small and medium-sized (< 10,000 population equivalent) and around 40% are equipped by nature-based processes such as constructed wetlands (CWs) [4]. These plants have different human and technical resources and therefore different needs compared to large-scale urban WWTPs. They require cheap, reliable and low-maintenance processes. Among the existing treatments for micropollutants, photoactivated advanced oxidation processes (AOPs) seem to meet these criteria. They consist in the generation of highly oxidising species such as $HO^{\bullet}$ ($E^0_{HO^{\bullet}/HO^-}$ = 2.80 V/SHE at 25 °C) by the photolysis of an oxidant precursor (typically H_2O_2). The abilities of the UVC/H_2O_2 process

have been widely reported. Cédat et al. [5] observed the complete degradation of a mixture of three estrogens (5 µM each spiked in a WWTP effluent) and of their estrogenic activity and estimated the cost of the technology to be under 0.20 € m^{-3}. However, UVC radiation is generally produced by mercury lamps which are quite energy consuming. In the UVC/H_2O_2 process, Cédat et al. [5] estimated that electricity would represent from 14 to 38% of the total treatment cost. Moreover, H_2O_2 supply is another significant expenditure item since it was estimated to represent from 47 to 62% of the total cost.

With a view to optimising the efficiency/cost ratio of the AOP, alternatives to the UVC/H_2O_2 treatment were presented in the literature. For example, the abilities of $S_2O_8^{2-}$ as an oxidant precursor to generate two sulfate radicals ($SO_4^{\bullet-}$) ($E^0_{SO_4^{\bullet-}/SO_4^{2-}}$ = 2.5 – 3.1 V/SHE at 25 °C, depending on the solution pH) by photolysis have been widely shown [6, 7, 8].

Then, another alternative is the use of solar light as a UV source. Incident solar radiation on earth is a free and renewable energy, composed of 95% of UVA and 5% of UVB and it was previously reported in the literature that UVA radiation is able to photolyse H_2O_2 and $S_2O_8^{2-}$ [9, 10]. Fernandes et al. [11] also recently demonstrated that natural solar radiation is efficient in activating these oxidant precursors. Kowalska et al. [12] and Moreira et al. [10] observed complete degradation of carbamazepine and diclofenac in spiked effluents under solar radiation coupled to H_2O_2. Finally, Rizzo et al. [13] and Velo-Gala et al. [14] both compared the efficiency of a solar simulator to UVC radiation for the activation of H_2O_2 in order to degrade antibiotics in small volumes (0.5 and 6 L respectively). In both studies, the lower efficiency of solar light compared to UVC radiation was concluded. However, the reported degradation rates were time-dependent and no comparison of the energy required (UV fluence) in each process was made.

Since UVA radiation constitute the majority of solar UV, it seems essential to evaluate their abilities for the activation of oxidant precursors in AOPs. To the best of our knowledge, no

previous study has compared UVA to UVC radiation for the photo-activation of H_2O_2 and $S_2O_8^{2-}$.

In the present work, an intermediate-scale laboratory pilot (maximum capacity of 50 L) was used to compare UVA to UVC radiation for the activation of H_2O_2 or $S_2O_8^{2-}$. H_2O_2 was chosen for its ease of implementation and the large number of studies identified in the literature. $S_2O_8^{2-}$ was studied for its high efficiency with the aim of assessing whether its use could balance the expected loss of efficiency when replacing UVC by UVA radiation. For technical reasons, mercury lamps were used for the production of both types of radiation, allowing UV fluence calculation and comparison. Three estrogens, namely estrone (E1), 17β-estradiol (E2) and 17α-ethinylestradiol (EE2), were first chosen as model pollutants for process efficiency assessment. According to Ilyas and van Hullebusch [15], they are removed from 30 to 80% in constructed wetlands, due to biodegradation, plant uptake and adsorption, leading to concentrations from ng L^{-1} to several µg L^{-1} in the released effluent. Similar degradation rates are also achieved in conventional WWTPs [16, 17]. Nevertheless, their occurrence in surface waters and river sediments as well as their ecotoxicity at environmental concentrations have been widely reported [18]. Finally, a mixture of ibuprofen, (IBU), naproxen (NAP) and diclofenac (DCF), three commonly detected non-steroidal anti-inflammatory drugs, allowed to confirm the results on another type of micropollutants.

2. Materials and methods

2.1. Chemicals and reagents

Estrone (E1), 17β-estradiol (E2), 17α-ethinylestradiol (EE2), ibuprofen (IBU) sodium salt, diclofenac (DCF) sodium salt and naproxen (NAP) were purchased from Sigma-Aldrich, as well as H_2O_2 (30% in water) and $Na_2S_2O_8$. Persulfate stock solutions were prepared in drinking water (1 M). E1, E2, EE2 and NAP stock solutions were prepared at 5 mM in acetonitrile. IBU and DCF stock solutions were made at 10 mM in drinking water.

Acetonitrile (ACN) was supplied by VWR Chemicals (HPLC grade). Ultrapure water was obtained from a milli-Q system. Formic acid was purchased from Chimie-plus Laboratoires.

2.2. Irradiation experiments

2.2.1. Description of the laboratory pilot

The experimental set-up has previously been described in the literature (Cédat et al., 2016) and is reproduced Figure 1. It is composed of a 50-L glass tank linked to a 1.12-L UV reactor (COMAP) by a centrifugal pump. In the reactor, the UV lamp is protected by a quartz tube and the effluent flows through a 1-cm layer around the tube. Effluent recirculation allows to increase the contact time between the targets and the lamp and thus the UV fluence. Low pressure mercury lamps (Philips) were used for the generation of UVC and UVA radiation. The UVC lamp was monochromatic while the UVA lamp was polychromatic and emits from 345 to 410 nm with a maximum at 365 nm (Figure SM1). Their technical features are presented in Table 1.

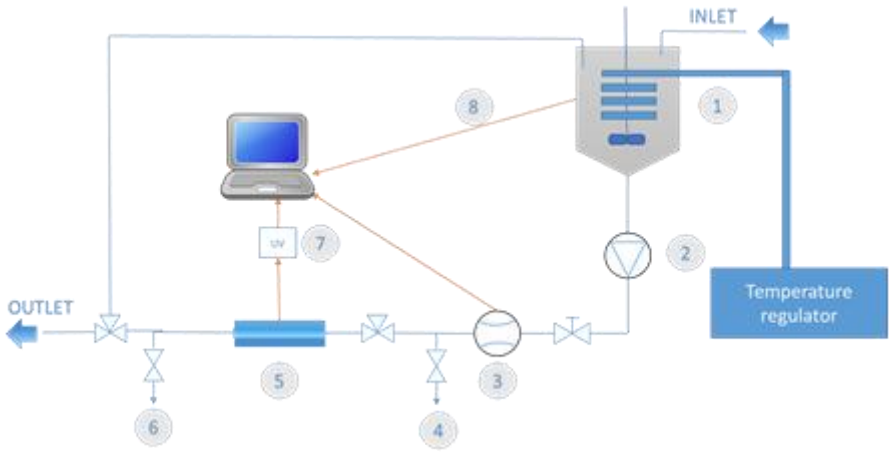

Figure 1. Schematic diagram of the pilot used, reproduced from Cédat *et al*., 2016. 1) Glass tank; 2) pump; 3) flow meter; 4) and 6) sampling points; 5) UV reactor; 7) UV intensity control; 8) temperature control.

Table 1. Technical characteristics of UVA and UVC lamps.

UV type	Lamp power (W)	Power efficiency	Wavelength (nm)	Length (cm)	Hg (mg)
UVC	54	32%	254	60.0	8.0
UVA	36	24%	345 – 410	89.5	2.0

The UVCalc®2A software (Bolton Photosciences Inc., Canada) was used for UV fluence calculations. On the advice of the software designer and given its narrow emission spectra, the UVA lamp was considered monochromatic. After calculation, a correction factor of 0.88 for UVC radiation [5] and 0.82 for UVA radiation (software designer recommendations) was applied.

2.2.2. Matrix composition

Main physico-chemical parameters of the matrices used to investigate the degradation of micropollutants are presented in Table 2. Drinking water collected directly to tap (Villeurbanne, France) was first used as a simple matrix. Then, WWTP effluents were collected in 30-L plastic containers at the outlet of a conventional WWTP equipped by an activated sludge treatment (Feyssine, Villeurbanne, France) with a capacity of 300,000 population equivalent. Samples were collected in the morning and used within 30 hours.

Table 2. Main physico-chemical parameters of drinking water and WWTP effluents.

	Drinking water	WWTP effluent 1	WWTP effluent 2
pH	7.7	7.8	7.9
UV_{254nm} transmittance	98%	62%	61%
UV_{365nm} transmittance	> 99%	90%	87%
Conductivity ($\mu S\ cm^{-1}$)	395	913	912
Suspended solids ($mg\ L^{-1}$)	-	4	4
Chemical Oxygen Demand (COD) ($mg\ L^{-1}$)	< 5	29	26
Total Organic Carbon (TOC) ($mg_C\ L^{-1}$)	-	7.5	5.8
Cl^- ($mg\ L^{-1}$)	10	107	98
NO_3^- ($mg\ L^{-1}$)	5.1	21.2	24.6
HCO_3^- ($mg\ L^{-1}$)	220	208	252

2.2.3. Experimental procedures

The laboratory pilot was used to determine the photolysis constants of the oxidant precursors, the photolysis first order rate constants of the estrogens and the overall pseudo-first order degradation rate constant of the estrogens or of the pharmaceuticals obtained through the experiments. Experimental procedures were quite similar and operating conditions are

summarized in Table 3. The experimental set-up was filled in to 20 ± 0.5 L with the matrix. Then, recirculation flow was set at 20 ± 0.5 L min^{-1}, the UV lamp was pre-heated during 10 minutes and the temperature was adjusted and stabilised at 22 ± 2 °C. After pre-heating, the lamp was turned off and the solution was spiked with 3 estrogens or 3 pharmaceuticals at 5 µM each (except for the experiments regarding oxidant precursor photolysis). Although this concentration is higher than those in WWTP effluents, it does not require pre-concentration prior to ultra high-performance liquid chromatography (UHPLC) analysis and therefore allows the sampling of small volumes, suitable for kinetic experiments. Then, an appropriate volume of oxidant precursor was added: 10.3 mL of H_2O_2 (30%) or 100 mL of a 1 M $S_2O_8^{2-}$ stock solution were added to reach a concentration of 5 mM ; 2.06 mL of H_2O_2 (30%) and 20 mL of $S_2O_8^{2-}$ 1 M were added to reach a concentration of 1 mM. No oxidant precursor was added for estrogen photolysis experiments. For oxidant precursor photolysis only, 100 mL of methanol (0.5% v/v) were also added: methanol quenches the newly formed hydroxyl or sulfate radicals to prevent them from reacting in turn with H_2O_2 or $S_2O_8^{2-}$.

After addition of the reagents, the solution was homogenised for 2 minutes and the lamp was turned on to start the experiment. 5 mL were withdrawn before the start and at the end of each experiment to measure the transmittance of the solution by UV-visible spectrophotometry. During estrogen photolysis and AOP experiments, 1 mL of sample was withdrawn at fixed time intervals for micropollutant quantification by UHPLC. During H_2O_2 or $S_2O_8^{2-}$ photolysis experiments, the volume of samples was extended to 5 mL to determine their concentrations using a UV-visible spectrophotometer.

In any case, variations between the initial and the final volume were under 0.25% during experiments.

Table 3. Operating conditions in the pilot.

	Photolysis experiments		UV-based AOP experiments	
	Oxidant precursors	Estrogens	Estrogens	Pharmaceuticals
Total volume	20 ± 0.5 L			
Recirculation flow rate	20 ± 0.5 L min^{-1}			
Solution	Drinking water	Drinking water	Drinking water or WWTP1	WWTP2
Micropollutants	None	E1 + E2 + EE2 5 µM each	E1 + E2 + EE2 5 µM each	IBU + NAP + DCF 5 µM each
Oxidant precursor	H_2O_2 or $S_2O_8^{2-}$ 5 mM	None	H_2O_2 or $S_2O_8^{2-}$ 1 mM	H_2O_2 or $S_2O_8^{2-}$ 1 mM
Methanol	0.5% V/V	None	None	None

2.3. Sample analysis

2.3.1. UV-visible spectrophotometry

A Shimadzu 2450 UV-visible spectrophotometer was used to:

- measure transmittances at 254 nm and 365 nm (required for UV fluence calculation),

- acquire the UV-visible spectra of the micropollutants and of the oxidant precursors,

- quantify H_2O_2 and $S_2O_8^{2-}$ during photolysis constant determination, using measurements carried out at 240 nm (ε_{240nm} = 38.1 L mol^{-1} cm^{-1}) and 230 nm (ε_{230nm} = 38.6 L mol^{-1} cm^{-1}) for H_2O_2 and $S_2O_8^{2-}$ respectively.

2.3.2. Micropollutant quantification

Samples were filtered before analysis through 0.45 µm PVDF filters (Millex HV). Analysis were performed with an UHPLC ultimate 3000+ (Thermo Fischer) system equipped with a X-Bridge BEH column (75 × 4.6 mm × 2.5 µm) and coupled to a diode array detector. The mobile phase was a mixture of acetonitrile (ACN) and milli-Q water both acidified with 0.1% formic acid running in isocratic mode at 1.5 mL min^{-1}. One method was used to analyse the estrogens and another to analyse the mixture of pharmaceuticals. They are both described in Table 4. Limits of detection (LOD) were determined by calculation and limits of

quantification were calculated as 3.3 × LOD. All the samples were analysed in duplicate. Examples of typical chromatograms are available in Figure SM2.

Table 4. UHPLC method parameters for micropollutant quantification.

UHPLC method	Estrogen method			Pharmaceutical method		
Pollutant	E1	E2	EE2	IBU	NAP	DCF
Mobile phase ACN/H_2O	50/50			60/40		
Injection volume (µL)	40			20		
Column temperature (°C)	40			40		
Detection wavelength (nm)	280			226	226	281
Retention times (min)	1.91	1.44	1.71	2.02	1.17	1.76
Limit of detection (µM)	0.28	0.25	0.26	0.12	0.10	0.09

2.4. Data processing

2.4.1. UV fluence

UV fluence (F, mJ cm^{-2}) corresponds to the total radiant energy incident from all directions onto an infinitesimally small sphere of cross-sectional area dA, divided by dA according to Bolton and Stefan [19]. In the studied system, the infinitesimally small sphere of cross-sectional area can be considered to be the targeted micropollutants or the oxidant precursors. UV fluence is based on the characteristics of the lamp but also on the structure of the system and on the transmittance of the effluent. Thus, it allows to compare different lamps, processes or effluents. In the present study, UV fluence was used as a reference unit for degradation rates.

2.4.2. Degradation rate constants

Photolysis of the estrogens and of the oxidant precursors followed first order rates that were fitted by the following equation: $\ln \frac{C}{C_0} = -k'_p F$, where C_0 and C are respectively the initial concentration and the concentration at UV fluence F of the compound of interest (µM) and k'_p the photolysis first order rate constant (cm^2 mJ^{-1}) which depends on the UV fluence received by the effluent.

In AOPs, micropollutant degradation followed pseudo-first order rates. Targets can be degraded by both photolysis and oxidation by the free radicals. In the present study, the

198 radicals are $HO^{\cdot}$ or $SO_4^{\cdot-}$, generated by the homolytic cleavage of H_2O_2 or $S_2O_8^{2-}$ respectively
199 (each of them generates two identical radicals). The two modes of degradation can be
200 distinguished in the following pseudo-first order rate equation, as proposed by Sharpless et
201 Linden [20] :
202 $\ln \frac{C}{C_0} = -(k'_p + k'_{ox})F = -k'F$, where k'_{ox} is the pseudo-first order rate constant of
203 radical-based oxidation and k' is the overall pseudo-first order rate constant. k'_{ox} depends on
204 both the steady-state concentration of the radical and on the second order reaction rate
205 between the oxidative radical and the compound of interest [21]. In the present study, k'
206 values were determined from UV-based AOP experiments and k'_{ox} values were calculated as
207 the difference between k' and k'_p.
208 The error bars associated to degradation constants equal to 3σ, derived from the scattering of
209 the experimental data around the fit curves (intra-series variability).
210 *2.4.3. Electrical energy per order*
211 The Electrical Energy per Order (E_{EO}) is the electrical energy (kWh) necessary to reduce the
212 concentration of a contaminant by one order of magnitude in one m^3 of effluent [22] (Bolton
213 *et al.*, 2001). It is often calculated according to the following equation [23, 24]: $E_{EO} =$
214 $\frac{P \cdot t \cdot 1000}{V \cdot \log\left(\frac{C_i}{C_f}\right)}$, where P is the lamp power (kW), t is the time of irradiation (h), V is the volume of
215 treated effluent (L), C_i and C_f are the initial and final concentrations of the target molecule
216 (expressed in µmol L^{-1} in this paper). This quantity is a useful indicator for comparing
217 photoactivated processes. It is generally considered that a photoactivated process may be
218 economically feasible if its E_{EO} value is less than 10 kWh m^{-3} $order^{-1}$ [25].
219 Experimental data used to calculate E_{EO} can be seen in Table SM1, only E_{EO} values are
220 presented in the Results and discussion section.
221 **3. Results and discussion**

3.1. Estrogen and oxidant precursor photolysis

The molar absorption coefficient (ε_λ) and the quantum yield (Φ_λ) are the two parameters that account for the photolysis efficiency of a compound. The molar absorption coefficient governs the absorption of a photon by the molecule at the wavelength of interest and the photolysis quantum yield (number of photolysed molecules divided by the number of photons absorbed) depends on the photochemical change that follows photon absorption [26]. Thus, the photolysis quantum yield influences the quantum yield for the generation of photolysis by-products. In the present paper, the modelling of degradation kinetics is not based on these two parameters, but they are used to comment qualitatively on the degradation constants calculated from experimental data.

Molar absorption coefficients of H_2O_2 and $S_2O_8^{2-}$ and of the targeted estrogens (E1, E2 and EE2) within the UV range are depicted in Figure 2. Molar absorption coefficients at the wavelengths of interest and quantum yields for the production of $HO^\bullet$ and $SO_4^{\bullet-}$ (from H_2O_2 and $S_2O_8^{2-}$ photolysis, respectively) found in the literature are reported in Table 5. No quantum yield values for the production of both radicals at 365 nm (maximum emission wavelength of the UVA lamp) were found in the literature, so the values reported in Table 5 correspond to the wavelength found closest to 365 nm, i.e. 351 nm. As shown by Hermann (2007), quantum yield decreases with increasing the wavelength of the photolysis light. This decrease is barely noticeable in the case of $HO^\bullet$ formation with quantum yield values from 1.0 to 0.96 when wavelength varies from 254 to 351 nm while it is much more significant in the case of $SO_4^{\bullet-}$ formation with quantum yield values from 1.4 to 0.5 in the same range of wavelength. It can therefore be assumed that $\Phi_{365nm}(HO^\bullet) \simeq \Phi_{351nm}(HO^\bullet)$ while $\Phi_{365nm}(SO_4^{\bullet-}) < \Phi_{351nm}(SO_4^{\bullet-})$ so that the ratio $\Phi_{365nm}(HO^\bullet)/ \Phi_{365nm}(SO_4^{\bullet-})$ can be considered greater than 1.9 for the comparison of quantum yields for the two radicals under UVA. Under UVC, the ratio $\Phi_{254nm}(HO^\bullet)/ \Phi_{254nm}(SO_4^{\bullet-})$ equals 0.8.

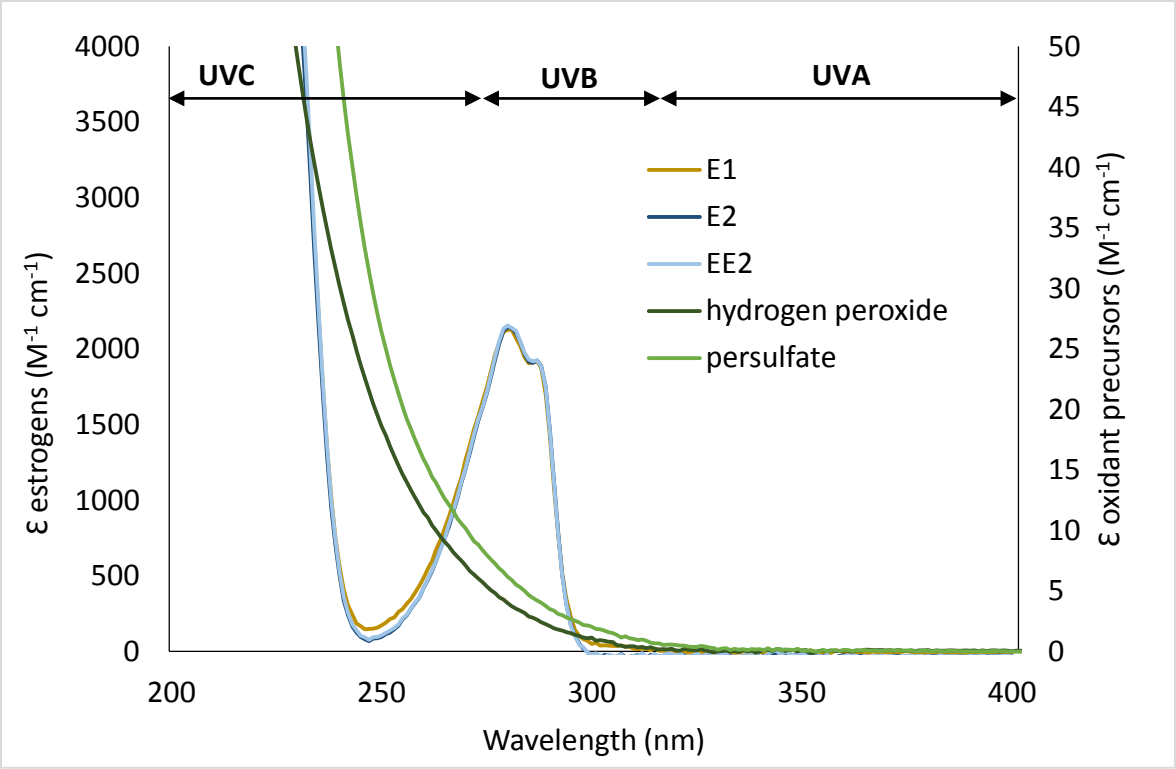

Figure 2. Molar absorption coefficients (Ɛ) of E1, E2 and EE2 and of H_2O_2 and $S_2O_8^{2-}$ in the UV range at circumneutral pH.

Table 5. Molar absorption coefficients (Ɛ) of estrogens and oxidant precursors and quantum yields for radical production (Φ) from the photolysis of oxidant precursors under UVC and UVA.

	Ɛ (M^{-1} cm^{-1})						Φ (mol ein^{-1})	
	H_2O_2	$S_2O_8^{2-}$	E1	E2	EE2		$HO^{\cdot}$	$SO_4^{\cdot-}$
UVA (365 nm)	< 0.3	< 0.5	< 10	< 10	< 10	UVA (351 nm)	0.96 ± 0.04[27]	0.5 ± 0.1[27]
UVC (254 nm)	15.4	21.3	261	175	175	UVC (254 nm)	1.15 ± 0.05[28]	1.4 ± 0.1[29]

3.1.2. Photolysis rate constants of the oxidant precursors

As seen in Figure 2, molar absorption coefficients follow the same trend in the UV range for both H_2O_2 and $S_2O_8^{2-}$: they are not significant between 400 and 350 nm and increase exponentially from 350 to 200 nm. According to Table 5, both oxidant precursors allow higher quantum yields for the production of free radicals under UVC than under UVA radiation. Therefore, although it was reported in the literature that UVA radiation is efficient

for their activation [9, 30], faster photolysis is expected under UVC radiation for both molecules.

At 254 nm, the molar absorption coefficient of $S_2O_8^{2-}$ is 1.4 times higher than that of H_2O_2 and the quantum yield for the production of $SO_4^{\bullet-}$ is 1.2 times higher than that of $HO^{\bullet}$ (Table 5). Therefore, faster production of $SO_4^{\bullet-}$ is expected. At 365 nm, a higher quantum yield for the production of $HO^{\bullet}$ is expected compared to $SO_4^{\bullet-}$, as suggested by values reported in the literature at 351 nm. However, molar absorption coefficients were too low to be determined, not allowing for the assessment of photolysis outcomes.

Photolysis first order rate constants of H_2O_2 and $S_2O_8^{2-}$ in the experimental facility are reported in Table 6. As expected, they are higher under UVC than under UVA radiation (3.5 and 8.8 times for H_2O_2 and $S_2O_8^{2-}$ respectively), causing faster generation of the subsequent free radicals under UVC radiation. The photolysis of $S_2O_8^{2-}$ is about 1.2 and 3.4 times faster than that of H_2O_2, under UVA and UVC radiation respectively. Therefore, the generation of $SO_4^{\bullet-}$ is expected to be faster than that of $HO^{\bullet}$ regardless of the wavelength.

Table 6. Photolysis first order rate constants (k'_p) of H_2O_2 and $S_2O_8^{2-}$ in the system.

	k'_p (cm^2 mJ^{-1})	
	H_2O_2	$S_2O_8^{2-}$
UVA	$4.36 \pm 0.30 \times 10^{-5}$	$5.25 \pm 0.51 \times 10^{-5}$
UVC	$1.54 \pm 0.02 \times 10^{-4}$	$4.61 \pm 0.26 \times 10^{-4}$

3.1.3. Photolysis of the estrogens

According to Figure 2, E1, E2 and EE2 molar absorption coefficients are very similar at all wavelengths. They have a similar absorption band from 300 to 250 nm and molar absorption coefficients increase exponentially in a similar way from 250 to 200 nm. However, at 254 nm, Ɛ is 1.5 times higher for E1 than for E2 and EE2. Moreover, according to Huang et al. [31], E1 has a 3 to 4 time higher quantum yield than E2 and EE2 at 254 nm. Therefore, faster photolysis of E1 is expected compared to that of E2 and EE2 at this wavelength. At 365 nm,

molar absorption coefficients are not significant for the three estrogens and to the best of our knowledge, their quantum yields at this wavelength were not reported in the literature.

Table 7 depicts the first order rate constants of E1, E2 and EE2 in the pilot (experimental data in the form of C/C_0 curves can be seen in Figure SM3 and Figure SM4 for UVA and UVC respectively). First of all, the estrogens were photolysed under UVA radiation despite very low molar absorption coefficients. Constants are of the same order of magnitude for the three estrogens, ranging from 8.4×10^{-6} to 1.9×10^{-5} cm^2 mJ^{-1} for E1 and EE2 respectively. They reflect very slow photolysis and less than 2% of the initial concentrations are degraded at 1000 $mJ.cm^2$, the maximum relevant UV fluence in AOPs [32], corresponding to 41 min in the pilot. Then, higher photolysis rates of the three estrogens were observed under UVC radiation. E2 and EE2 photolysis are 3 to 4 times faster and that of E1 is 113 times faster. As seen previously, faster photolysis of E1 under UVC radiation was expected given its higher ε_{254nm} and Φ_{254nm} values. Nevertheless, the photolysis remains slow under UVC radiation with only 3 to 4% degradation for E2 and EE2 at 1000 mJ cm^2, whereas E1 was degraded by 62%. If photolysis may take part in the global degradation of estrogens during AOPs, UV irradiation cannot be considered as an effective treatment, whether it is under UVA or UVC radiation.

Table 7. Photolysis of E1, E2 and EE2 in the system: k'_p and E_{EO} values.

		E1	E2	EE2
k'_p (cm^2 mJ^{-1})	UVA	$8.4 \pm 3.0 \times 10^{-6}$	$1.2 \pm 0.2 \times 10^{-5}$	$1.9 \pm 0.1 \times 10^{-5}$
	UVC	$9.6 \pm 0.5 \times 10^{-4}$	$4.8 \pm 0.3 \times 10^{-5}$	$6.4 \pm 0.2 \times 10^{-5}$
E_{EO} (kWh m^{-3} $order^{-1}$)	UVA	424.8	223.5	145.9
	UVC	2.1	47.1	31.8

These considerations are confirmed by the values of E_{EO} reported in Table 7: with UVA, it takes between one hundred and four hundred kWh to reduce the concentration of each estrogen in a m^3 of drinking water by an order of magnitude, which far exceeds the energy

consumption compatible with economic feasibility. With UVC, lower E_{EO} values are obtained, of the order of several tens for E2 and EE2, which remains higher than the threshold value of 10 kWh m^{-3} $order^{-1}$, even if photolysis alone could be economically viable for E1 hormone degradation.

3.2. Estrogen degradation in drinking water in various AOPs

Pseudo-first order rate constants (k') of the estrogens in drinking water were calculated from experimental data (available as C/C_0 curves in Figure SM3 and Figure SM4 for UVA and UVC respectively) and are shown Table 8 as well as associated oxidation constants k'_{ox} calculated as the difference between k' and k'_p (reported in Table 7). The contribution of oxidation to the global degradation of the targets ($\%_{ox}$) was also calculated and is presented in Table 8, the complement to 100 corresponding to the contribution of photolysis.

Table 8. Pseudo-first order degradation constants (k') of E1, E2 and EE2 in the different processes with the associated oxidation constants (k'_{ox}) and their degradation rates at 1000 mj.cm^{-2}.

Radiation type	Oxidant precursor	Estrogen	Rate constants (cm^2 mJ^{-1})		$\%_{ox}$	Degradation at 1000 mJ cm^{-2} (%)
			k'	k'_{ox}		
UVA	H_2O_2	E1	2.2×10^{-5}	1.4×10^{-5}	64	2.2
		E2	3.3×10^{-5}	2.0×10^{-5}	61	3.2
		EE2	3.5×10^{-5}	1.6×10^{-5}	46	3.4
	$S_2O_8^{2-}$	E1	2.1×10^{-4}	2.1×10^{-4}	100	19
		E2	2.8×10^{-4}	2.7×10^{-4}	96	24
		EE2	3.0×10^{-4}	2.8×10^{-4}	93	26
UVC	H_2O_2	E1	1.7×10^{-3}	7.2×10^{-4}	42	81
		E2	9.4×10^{-4}	8.9×10^{-4}	95	61
		EE2	9.5×10^{-4}	8.9×10^{-4}	94	61
	$S_2O_8^{2-}$	E1	1.1×10^{-2}	1.0×10^{-2}	91	100
		E2	1.1×10^{-2}	1.1×10^{-2}	100	100
		EE2	1.1×10^{-2}	1.1×10^{-2}	100	100

Firstly, as expected, UVC radiation allows for 30 to 80% faster degradation, depending on the oxidant precursor and on the estrogen. k' ranges from $2.2 \pm 0.2 \times 10^{-5}$ to $3.0 \pm 0.2 \times 10^{-4}$ cm^2 mJ^{-1} under UVA and from $9.4 \pm 0.4 \times 10^{-4}$ to $1.1 \pm 0.1 \times 10^{-3}$ cm^2 mJ^{-1} under UVC radiation. Under UVA radiation, k' are ranked as follows regardless of the oxidant precursor: E1 < E2 < EE2. On the other hand, under UVC radiation, k' are similar in the presence of $S_2O_8^{2-}$ whereas it is almost twice as high for E1 than for E2 and EE2 in the presence of H_2O_2.

When comparing the oxidant precursors, k' are 7 to 12 times higher with $S_2O_8^{2-}$ than with H_2O_2 regardless of the UV type for E2 and EE2 and under UVA only for E1. Under UVC radiation, k'_{E1} is only about 5 times faster with $S_2O_8^{2-}$ than with H_2O_2.

In the UVA/H_2O_2 process, k' goes from $2.2 \pm 0.2 \times 10^{-5}$ to $3.5 \pm 0.3 \times 10^{-5}$ cm^2 mJ^{-1} with 46 to 64% of the degradation achieved by oxidation. These close results are attributed to similar photolysis constants of the estrogens (Table 7) and similar second order rate constants (from 1.8 to 2.9×10^{10} M^{-1} s^{-1}) between $HO^{\cdot}$ and the estrogens [9]. When using $S_2O_8^{2-}$, k' values increase by 89 ± 1% and are similar between the estrogens, ranging from 2.1 to 3.0×10^{-4} cm^2 mJ^{-1}, due to close second order rate constants (from 1.8 to 4.1×10^9 M^{-1} s^{-1}) between $SO_4^{\cdot-}$ and the estrogens [9]. This increase is attributed to higher k'_{ox} thanks to faster photolysis of $S_2O_8^{2-}$ compared to H_2O_2 (× 1.2) (see Table 6). As a consequence, the contribution of oxidation increases, being equal to or greater than 93%.

Under UVC radiation, the degradation of the estrogens is accelerated. In the presence of H_2O_2, k' are from 27 to 77 times higher than those obtained under UVA. In addition to faster estrogen photolysis, H_2O_2 photolysis is 3.5 times faster under UVC than under UVA (Table 7). k'_{E2} and k'_{EE2} are similar with a contribution of oxidation reaching 95 and 94% respectively. However, k'_{E1} is almost twice as high as k'_{E2} and k'_{EE2}. It is observed that k'_{ox} are

of the same order of magnitude for the three estrogens, from 7.2 to 8.9×10^{-4} cm^2 mJ^{-1}. Therefore, faster degradation of E1 is attributed to its high photosensitivity under UVC radiation. Similar trends are observed with the use of $S_2O_8^{2-}$: k' are from 39 to 52 times higher under UVC radiation due to faster oxidation. For E2 and EE2, the increase in k'_{ox} is so high that k'_p becomes negligible. Regarding E1, k'_p remains noticeable (about 10% of total degradation). However, a lower k'_{ox} leads to similar k' than that of E2 and EE2. Finally, oxidation plays a major role in E2 and EE2 degradation under UVC regardless of the oxidant precursor whereas the predominant phenomenon in the degradation of E1 varies depending on the oxidant precursor.

Estrogen degradation rates at 1000 mJ cm^{-2} are reported in Table 8. With UVC/$S_2O_8^{2-}$, the three estrogens are fully degraded. On the other hand, the UVA/H_2O_2 process provides less than 4% degradation at 1000 mJ cm^{-2} and does not seem viable. As a consequence, it was not studied in the following parts of the work. Contrasted results are observed with UVA/$S_2O_8^{2-}$ (19 to 26% degradation) and UVC/H_2O_2 (61 to 81% degradation). With the aim of promoting the use of UVA rather than UVC radiation in photoactivated AOPs, coupling UVA radiation to $S_2O_8^{2-}$ could be relevant since it induces encouraging results compared to the UVC/H_2O_2 process.

The values of E_{EO} calculated for estrogens degradation in drinking water shown in Table 9 lead to the same conclusions. Using UVC whatever the free radical precursor seems to be economically feasible with E_{EO}values between 0 and 2 kWh m^{-3} $order^{-1}$. So it seems worthwhile to study the UVC-based AOPs with a complex matrix such as WWTP effluent, even if these conditions may be less favorable. With the UVA/$S_2O_8^{2-}$ process, E_{EO} values are a little bit higher, in the upper range of acceptable values. It is therefore important to determine whether the switch to real matrix leads to a significant increase in E_{EO} values or not. Finally,

E_{EO} values obtained with the UVA/H_2O_2 process are around hundred for the three estrogens in drinking water, so there is no point in going any further with this process.

Table 9. Values of E_{EO} for estrogens degradation by photooxidation in different matrices.

Radiation type	Oxidant precursor	Estrogen	E_{EO} (kWh m^{-3} $order^{-1}$)		Ratio $\frac{E_{EO}(DW)}{E_{EO}(WWTP)}$
			Drinking water	WWTP effluent	
UVA	H_2O_2	E1	126.6	-	-
		E2	81.3	-	-
		EE2	84.4	-	-
	$S_2O_8^{2-}$	E1	10.3	59.8	5.8
		E2	7.6	55.1	7.2
		EE2	7.3	49.4	6.7
UVC	H_2O_2	E1	1.3	2.1	1.6
		E2	2.2	3.5	1.6
		EE2	2.1	3.2	1.5
	$S_2O_8^{2-}$	E1	0.2	0.9	5.0
		E2	0.1	0.9	7.7
		EE2	0.1	0.9	7.1

3.3. Process comparison in a WWTP effluent

After the study of UV-based AOPs in a simple matrix, it is necessary to implement them in a real matrix. Real effluents may indeed contain species that absorb UV radiations, react with radical precursors and/or with free radicals, leading to poorer performance of the process. Furthermore, it has been shown that photolysis and oxidation are compound dependent. Thus, it seems interesting to assess the degradation of another kind of micropollutants. This part, dedicated to the degradation of micropollutants in spiked WWTP effluents, firstly focuses on the estrogens and then on a mixture of three pharmaceuticals.

3.3.1. Estrogen degradation

WWTP effluent 1 collected at the outlet of a conventional treatment plant (see Table 2 for more details) and spiked with the three estrogens was used to assess the performance of the UVA/$S_2O_8^{2-}$, UVC/H_2O_2 and UVC/$S_2O_8^{2-}$ processes (see Table 3 for operating conditions).

Pseudo-first order degradation rate constants of the estrogens are presented and compared to those measured in drinking water in Figure 3 (data is available in Table SM2, experimental data is available as C/C_0 curves in Figure SM5).

First of all, estrogen degradation rates in WWTP effluent follow the same behaviours as described previously in drinking water: $S_2O_8^{2-}$ induces faster degradation than H_2O_2 and UVC is more efficient than UVA radiation (with $S_2O_8^{2-}$ only since UVA/H_2O_2 was not implemented). However, k' are lower in the WWTP effluent than in drinking water. Inhibition percentages are presented in Figure 3. They were calculated by comparing the degradation rate constants obtained in the WWTP effluent to those obtained in drinking water. In the presence of $S_2O_8^{2-}$ and regardless of the type of radiation, k' are reduced by 76 to 80%. However, in the UVC/H_2O_2 process, degradation rates are only inhibited by 27, 30 and 12% for E1, E2 and EE2 respectively. Based on these results, process performances seem to be much more affected in a real matrix when $S_2O_8^{2-}$ is used compared to H_2O_2.

In the literature, the reactivity of H_2O_2 and $S_2O_8^{2-}$ with the WWTP effluent components (mainly organic matter and inorganic anions) was not reported to be significant. The inhibition in a WWTP effluent is rather probably due to the scavenging of the oxidative radicals by the organic matter and inorganic anions such as Cl^-, NO_3^- and HCO_3^- [9, 33, 34]. Results obtained in the present study suggest that the scavenging of the radicals by the matrix components is stronger for $SO_4^{\bullet-}$ than for $HO^\bullet$. In both matrices under study, carbonate concentrations are similar. However, the total organic carbon of the effluent is 7.5 $mg_C\ L^{-1}$ whereas that of drinking water is not significant (< 0.5 $mg_C\ L^{-1}$). In addition, conductivity, chloride and nitrate concentrations are 2.3, 10 and 4.2 times higher in the WWTP effluent respectively. These differences in matrix composition could indeed induce $HO^\bullet$ and $SO_4^{\bullet-}$ scavenging. Wang and Wang [35] reported in a literature review that both radicals have similar second order reaction rate constants with HCO_3^- ($9 \times 10^6\ M^{-1}\ s^{-1}$), that Cl^- have

407 negligible effect and that NO_3^- could have a scavenging impact, although its second order
408 reaction rate with HO· is not reported and that with $SO_4^{\cdot -}$ is negligible
409 ($k''_{SO_4^{\cdot -},NO_3^-}$ = 2.1 M^{-1} s^{-1}). Therefore, the significant decrease in efficiency of $S_2O_8^{2-}$ observed
410 in the present study under both types of radiation could rather be attributed to radical
411 scavenging by organic matter, which would be stronger for $SO_4^{\cdot -}$ than for HO·. This
412 inhibition is governed by the competition between the micropollutants of interest and organic
413 matter to react with the radicals. Second order rate constants between the radicals and the
414 organic matter were not determined in the present study. However, Lutze et al. [36] reported
415 higher reaction rates of natural organic matter with HO· than with $SO_4^{\cdot -}$ but they only
416 considered humic acids whereas it was previously reported in the literature that the
417 composition of organic matter in WWTP effluents has a large variation range which also
418 includes fulvic acids, hydrophilic acids, bases and neutral or hydrophobic neutrals for
419 example [37, 38, 39]. Regarding the reactivity between the estrogens and the radicals, Gabet
420 et al. [9] previously reported that second order rate constants are lower with $SO_4^{\cdot -}$ (from 1.8 ×
421 10^9 to 4.1 × 10^9 M^{-1} s^{-1}) than with HO· (from 1.8 × 10^{10} to 2.9 × 10^{10} M^{-1} s^{-1}). As a
422 consequence, $SO_4^{\cdot -}$ is more likely to be scavenged by organic matter than HO·, depending on
423 their second order reaction rates with the organic matter involved.

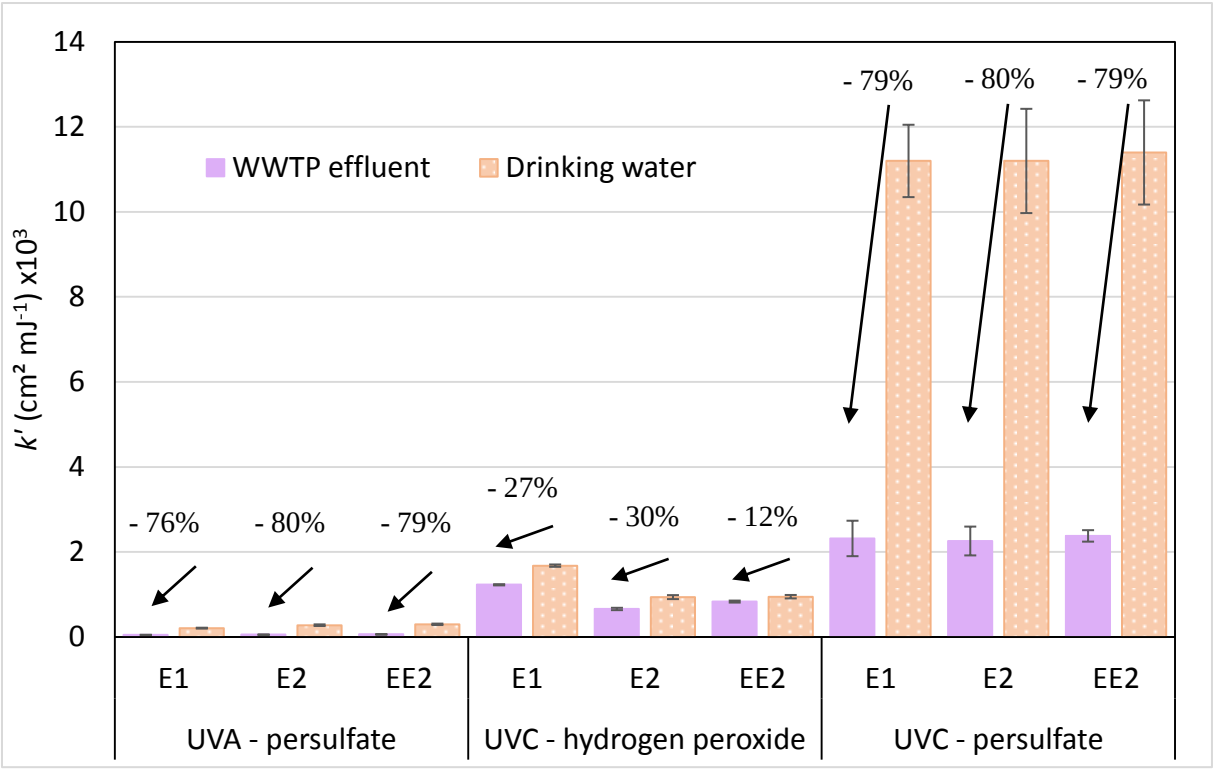

Figure 3. Pseudo-first order degradation rate constants of E1, E2 and EE2 (5 µM) in a WWTP effluent compared to those in drinking water, H_2O_2 or $S_2O_8^{2-}$ = 1 mM.

In drinking water, UVA/$S_2O_8^{2-}$ seemed to have potential in degrading estrogens: it induced degradation rates only 3 to 8 times slower than UVC/H_2O_2. In the WWTP effluent, this is no longer the case because UVA/$S_2O_8^{2-}$ provides 12 to 24 times lower k' values than UVC/H_2O_2.

Regarding UVC-based processes, UVC/$S_2O_8^{2-}$ was by far the most competitive process in drinking water with 7 to 12 times faster degradations than with H_2O_2. In a WWTP effluent, they are only 2 to 3.4 times faster than with H_2O_2. Therefore, even if UVC/$S_2O_8^{2-}$ still gives the best results, performance indicators become of the same order of magnitude as those obtained with UVC/H_2O_2.

Unsurprisingly, the E_{EO} values reported in Table 9 show that the electrical energy required to reduce estrogens concentrations by one order of magnitude increases when aqueous matrix becomes more complex (from drinking water to WWTP effluent). However, UVC-based processes still exhibit E_{EO} values lower than 10 kWh m^{-3} $order^{-1}$ and even lower than 4, attesting to their economic feasibility. Based on E_{EO}, UVC/$S_2O_8^{2-}$ is more attractive than

UVC/H_2O_2 with E_{EO} values two to four times lower. Regarding UVA/$S_2O_8^{2-}$ process, switching to a real matrix raises E_{EO} values (up to between 50 and 60 kWh m^{-3} $order^{-1}$) above the economic feasibility threshold. While this excess is not strictly prohibitive for UVA technologies, it does indicate that UVC-based AOPs are comparatively more economically attractive.

For the two processes that use persulfate ions as radical precursors, E_{EO} values increase by a factor of between 5 and 8 as a result of the matrix change, whether with UVA or UVC, whereas this factor is around 1.5 for UVC/H_2O_2. As seen above based on kinetics considerations, the switch to a real matrix also reduces the performance of persulfate based AOPs more than that of H_2O_2 based ones.

3.3.2. Pharmaceutical degradation

WWTP effluent 2 collected at the outlet of the same conventional treatment plant (see Table 2 for more details) was spiked with a mixture of three pharmaceuticals, namely ibuprofen (IBU), naproxen (NAP) and diclofenac (DCF). The UVA/$S_2O_8^{2-}$, UVC/H_2O_2 and UVC/$S_2O_8^{2-}$ processes were carried out in the same conditions as previously. Pseudo-first order degradation rates of the mixture of pharmaceuticals are depicted in Figure 4 (data is available in Table SM3 and experimental data is available as C/C_0 curves in Figure SM6).

In all the processes, k' are significantly different between the three compounds and their ranking is similar in the three processes: $k'_{IBU} < k'_{NAP} < k'_{DCF}$. k'_{DCF} is 7 and 11 times higher than k'_{IBU} with H_2O_2 and $S_2O_8^{2-}$ respectively and it is 5.5 times greater than k'_{NAP} with H_2O_2. However, it is less than twice k'_{NAP} with $S_2O_8^{2-}$. As observed for the estrogens, both UVC processes provide faster degradation rates than UVA/$S_2O_8^{2-}$ (from 10 to 63 times with H_2O_2 and from 38 to 56 times with $S_2O_8^{2-}$). However, degradation rates are of the same order of magnitude under UVC radiation with the two oxidant precursors. They are only 1.3 and 3.7

464 times faster with $S_2O_8^{2-}$ for DCF and NAP respectively and the degradation of IBU is on the
465 contrary 1.2 times slower with $S_2O_8^{2-}$ than with H_2O_2.
466 Firstly, the difference in degradation rates between the three pharmaceuticals is going to be
467 discussed. Under UVC radiation, DFC is highly photolysable: Fu et al. [40] reported a high
468 photolysis rate of DCF with 92% degradation after 600 s of exposure in their system whereas
469 NAP and IBU were degraded by 52 and 28% respectively. Under UVA radiation, low
470 photolysis is expected in view of the global degradation results reported in Figure 4.
471 However, it has not been studied, to the best of our knowledge. Regarding oxidation, second
472 order rate constants (k'') all are of the same order of magnitude (Table 10). However, they
473 follow the same trend as k': those of DCF are equal to or higher than those of NAP which are
474 higher than those of IBU. Therefore, the differences in pseudo-first order degradation rates
475 between the pharmaceuticals are attributed to both their different photo-sensitivities and their
476 second order rate constants with HO· and $SO_4^{\cdot-}$.

477 Table 10. Second order reaction constants between the radicals and IBU, NAP and DCF.

	IBU	NAP	DCF
$k''_{HO\cdot}$ (M^{-1} s^{-1})	5.57×10^9 [41]	9.05×10^9 [42]	9.29×10^9 [43]
$k''_{SO_4^{\cdot-}}$ (M^{-1} s^{-1})	1.32×10^9 [41]	5.64×10^9 [42]	9.2×10^9 [44]

478

479 Regarding process efficiency, faster degradation under UVC radiation is attributed to both
480 faster pharmaceutical photolysis and radical generation. Moreover, as seen previously, better
481 degradation in the presence of $S_2O_8^{2-}$ is attributed to the faster generation of $SO_4^{\cdot-}$ compared
482 to HO·. Under UVC radiation, only the degradation of IBU is faster in the presence of H_2O_2
483 than with $S_2O_8^{2-}$. This is due to $k''_{HO\cdot,IBU}$ which is more than 4 times higher than $k''_{SO_4^{\cdot-},IBU}$.
484 The same trend is observed with NAP whose second order rate constant is 1.6 times higher
485 with HO· compared to $SO_4^{\cdot-}$. However, the competition between the different species or the

faster generation of $SO_4^{\bullet -}$ allows NAP to be degraded faster in the UVC/$S_2O_8^{2-}$ process compared to UVC/H_2O_2.

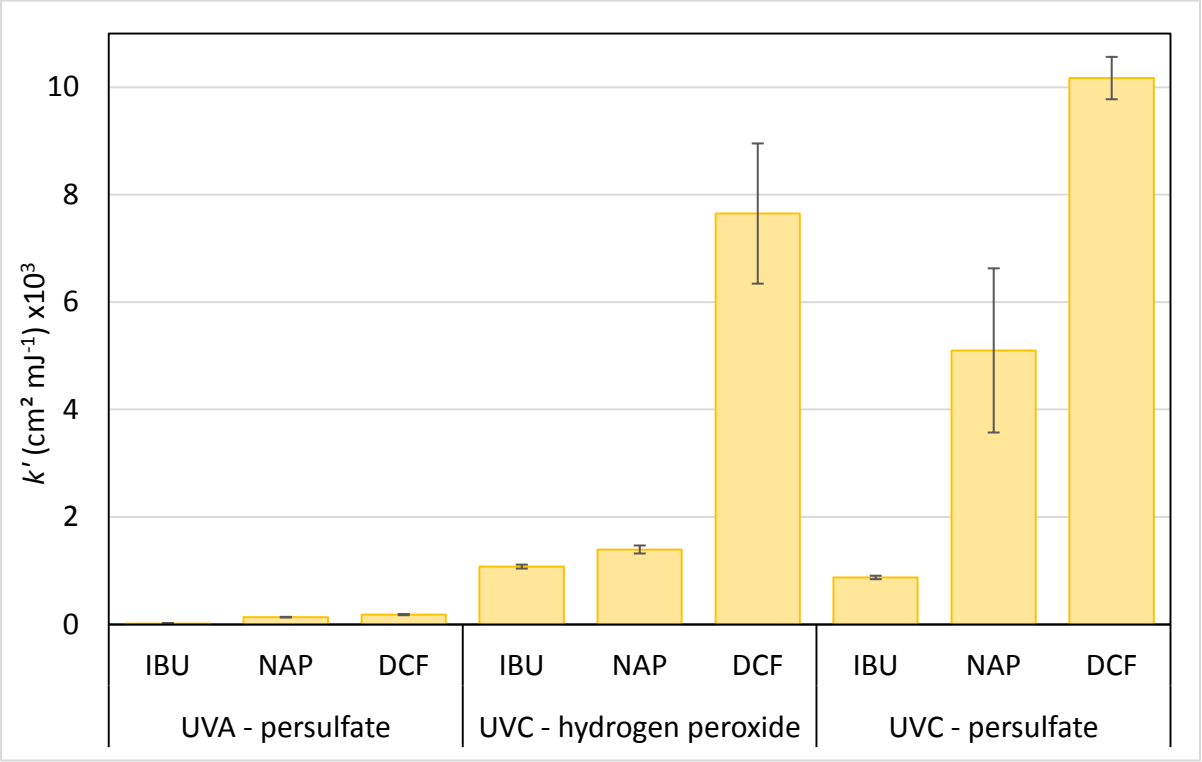

Figure 4. Pseudo-first order degradation rate constants of IBU, NAP and DCF (5 µM) in a WWTP effluent, H_2O_2 or $S_2O_8^{2-}$ = 1 mM.

E_{EO} calculated for the degradation of pharmaceuticals are shown in Table 11. As already seen with estrogens, UVC-based AOPs exhibit more favorable values of E_{EO} (lower than 10 kWh m^{-3} order$^-$) than UVA-based one. With persulphate ions as radical precursor and irrespective of UV radiation energy, the E_{EO} of IBU is significantly higher than that of NAP and DCF, which are of the same order of magnitude. E_{EO} obtained from UVC/H_2O_2 experiments are less contrasted. It is worth noticing that when comparing the highest and the lowest E_{EO} values for a given AOP, the ratios vary from 7 to 20 in the case of pharmaceuticals attesting a high degree of variability depending on the molecules, whereas they were much less dispersed, from 1.4 to 2.0, in the case of hormones which have fairly similar molecular structures.

Table 11. Values of E_{EO} for pharmaceuticals degradation by photooxidation in WWTP effluent 2.

Radiation type	Oxidant precursor	Pharmaceutical	E_{EO} (kWh m^{-3} $order^{-1}$)
UVA	$S_2O_8^{2-}$	IBU	203.1
		NAP	23.3
		DCF	15.5
UVC	H_2O_2	IBU	2.1
		NAP	1.7
		DCF	0.3
	$S_2O_8^{2-}$	IBU	4.0
		NAP	0.5
		DCF	0.2

501

502 *3.3.3. Removal efficiencies at 1000 mJ cm^{-2}*

503 Removal efficiencies at 1000 mJ cm^{-2} in the three processes are depicted in Table SM2 for
504 estrogens and in Table SM3 for the pharmaceuticals.

505 The UVA/$S_2O_8^{2-}$ process only allowed weak degradation of the model micropollutants. The
506 estrogens were not degraded by more than 6% and the pharmaceuticals by 17%. On the other
507 hand, UVC radiation allowed satisfactory or good removal efficiencies at 1000 mJ cm^{-2},
508 depending on the model micropollutant and the oxidant precursor. In the presence of H_2O_2,
509 the estrogens were degraded from 43 to 71% and IBU, NAP and DCF were degraded by 66,
510 75 and 100% respectively. In the presence of $S_2O_8^{2-}$, the three estrogens underwent better
511 degradation with removal efficiencies reaching 90 ± 1%. NAP also underwent better
512 degradation and was almost completely degraded (99%) and DCF was still completely
513 removed, whereas IBU was only degraded by 58%, which is slightly poorer than the
514 degradation performances allowed by the UVC/H_2O_2 process, due to a lower k', as discussed
515 in section 3.3.2. As a consequence, the better performances of the UVC/$S_2O_8^{2-}$ are clear for
516 the estrogens and NAP. However, both UVC processes are comparable for the degradation of
517 DCF which is mainly photodegraded and IBU reaches slightly higher degradation in the

518 presence of H_2O_2, depicting the importance of the nature of the target in the process efficiency
519 assessment.

520 In Switzerland, where a regulation regarding the removal of micropollutants in WWTPs is
521 applicable, it imposes 80% removal on a selection of micropollutants over the complete
522 treatment process. In the present study, the UVC/$S_2O_8^{2-}$ process provides alone such
523 degradation for 5 of the 6 studied compounds and although the UVC/H_2O_2 process does not
524 allow such performances, it could significantly increase the overall micropollutant removal in
525 a WWTP when used as a tertiary treatment.

526 **4. Conclusion**

527 The following main conclusions can be drawn from this study about the feasibility of
528 replacing UVC by UVA in AOPs to degrade micropollutant. Firstly, experiments carried out
529 in drinking water as a simplified matrix with a mixture of estrogens showed that UVA is less
530 efficient than UVC in photolyzing both the radical precursors (H_2O_2 or $S_2O_8^{2-}$) and targeted
531 compounds, which results in lower degradation rates as well as poorer performance at a given
532 UV fluence. Based on E_{EO} calculations, UVA/H_2O_2 seems not economically feasible unlike
533 other AOPs.

534 Experiments carried out with estrogens- or pharmaceuticals-spiked WWTP effluents showed
535 that in the presence of a complex matrix, the UVA/$S_2O_8^{2-}$ process is no longer feasible with
536 values of E_{EO} higher than threshold value. For all AOPs, performance decreases drastically in
537 WWTP matrix, but the UVC-based processes remain economically feasible with satisfactory
538 micropollutant degradation. Persulphate ions still provide better degradation performances
539 than H_2O_2, even though inhibition due to matrix change, expressed as a % relative to drinking
540 water, is stronger, showing a higher scavenging effect of $SO_4^{\cdot -}$ than of $HO^{\cdot}$ by organic matter.

Since the efficiency of a radical precursor is both compound- and matrix-dependent, further experiments on a larger panel of micropollutants would be required in order to confirm $S_2O_8^{2-}$ better efficiency.

The E_{EO} is a useful tool to compare AOPs, and especially to compare UVA- and UVC-processes. Nevertheless, it should be completed by another parameter that would enable a fair comparison of radical precursors to be integrated in a technico-economical indicator. For example, the price of a reagent is not the only parameter that induces cost, its implementation has also to be taken into account. However, in view of the experiences carried out in the present study, a more detailed technical and economic approach seems premature.

Finally, if the use of mercury-based UVA lamps is ruled out by the results of the present study, there are other UVA radiation sources that could allow for the implementation of less energy consuming processes and for the consideration of UV fluences greater than 1000 mJ cm^{-2} (defined for UVC mercury-based lamps). UVA-light emitting diodes (LEDs) are one of them. LEDs have been an emerging light source over the past years and they are known for their high energy efficiency, robustness, clean composition and potential for long lifetimes [45]. UVA-LEDs are particularly interesting because they can be up to 15 times more energy efficient than UVA mercury lamps [46], on the contrary to UVC-LEDs which have low energy efficiency [47]. Another solution for UVA-based processes are solar-driven systems that would allow considering greater energy requirements to reach complete degradation of the targets because solar light is a free and clean energy. However, their major drawback remains process implementation: despite the availability of solar light concentrator, designing a system able to provide appropriate UV fluence for the degradation of micropollutants with solar radiation remains nowadays challenging.

5. Declaration of Competing Interest

All authors declare no conflict of interest.

Acknowledgements

The authors wish to acknowledge the financial support of the “Région Auvergne-Rhône-Alpes” for their financial support through the “Pack Ambition Recherche”. This work was performed within the framework of the EUR H2O’Lyon (ANR-17-EURE-0018) of Université de Lyon (UdL), within the program "Investissements d'Avenir” operated by the French National Research Agency (ANR). This work was also supported by the “Federation des Recherches en Environnement” through the CPER “Environnement” founded by the “Région Auvergne,” the French government and FEDER from European community.

References

[1] Gallé, T., Pittois, D., Bayerle, M., & Braun, C. (2019). An immission perspective of emerging micropollutant pressure in Luxembourgish surface waters : A simple evaluation scheme for wastewater impact assessment. *Environmental Pollution*, *253*, 992‑ 999. https://doi.org/10.1016/j.envpol.2019.07.080.

[2] Luo, Y., Guo, W., Ngo, H. H., Nghiem, L. D., Hai, F. I., Zhang, J., Liang, S., & Wang, X. C. (2014). A review on the occurrence of micropollutants in the aquatic environment and their fate and removal during wastewater treatment. *Science of The Total Environment*, *473‑ 474*, 619‑ 641. https://doi.org/10.1016/j.scitotenv.2013.12.065.

[3] Pasquini, L., Munoz, J.-F., Pons, M.-N., Yvon, J., Dauchy, X., France, X., Le, N. D., France-Lanord, C., & Görner, T. (2014). Occurrence of eight household micropollutants in urban wastewater and their fate in a wastewater treatment plant. Statistical evaluation. *Science of The Total Environment*, *481*, 459‑ 468. https://doi.org/10.1016/j.scitotenv.2014.02.075.

[4] *Portail assainissement collectif*. (s. d.). Consulté 12 septembre 2022, à l'adresse https://www.assainissement.developpement-durable.gouv.fr/PortailAC/liste_inc_new2

[5] Cédat, B., de Brauer, C., Métivier, H., Dumont, N., & Tutundjan, R. (2016). Are UV photolysis and UV/H2O2 process efficient to treat estrogens in waters? Chemical and biological assessment at pilot scale. *Water Research*, *100*, 357‑ 366. https://doi.org/10.1016/j.watres.2016.05.040.

[6] Chen, P.-J., Rosenfeldt, E. J., Kullman, S. W., Hinton, D. E., & Linden, K. G. (2007). Biological assessments of a mixture of endocrine disruptors at environmentally relevant concentrations in water following UV/H2O2 oxidation. *Science of The Total Environment*, *376*(1‑ 3), 18‑ 26. https://doi.org/10.1016/j.scitotenv.2006.12.051.

598 [7] Song, W., Li, J., Wang, Z., & Zhang, X. (2019). A mini review of activated methods to
599 persulfate-based advanced oxidation process. *Water Science and Technology*, *79*(3),
600 573‐ 579. https://doi.org/10.2166/wcc.2018.168.
601 [8] Zhang, W., Zhou, S., Sun, J., Meng, X., Luo, J., Zhou, D., & Crittenden, J. (2018). Impact
602 of Chloride Ions on UV/H $_2$ O $_2$ and UV/Persulfate Advanced Oxidation Processes.
603 *Environmental Science & Technology*, *52*(13), 7380‐ 7389.
604 https://doi.org/10.1021/acs.est.8b01662.
605 [9] Gabet, A., Métivier, H., de Brauer, C., Mailhot, G., & Brigante, M. (2021). Hydrogen
606 peroxide and persulfate activation using UVA-UVB radiation : Degradation of estrogenic
607 compounds and application in sewage treatment plant waters. *Journal of Hazardous*
608 *Materials*, *405*, 124693. https://doi.org/10.1016/j.jhazmat.2020.124693.
609 [10] Moreira, N. F. F., Narciso-da-Rocha, C., Polo-López, M. I., Pastrana-Martínez, L. M.,
610 Faria, J. L., Manaia, C. M., Fernández-Ibáñez, P., Nunes, O. C., & Silva, A. M. T. (2018).
611 Solar treatment (H2O2, TiO2-P25 and GO-TiO2 photocatalysis, photo-Fenton) of organic
612 micropollutants, human pathogen indicators, antibiotic resistant bacteria and related genes in
613 urban wastewater. *Water Research*, *135*, 195‐ 206.
614 https://doi.org/10.1016/j.watres.2018.01.064.
615 [11] Fernandes, C. H. M., Silva, B. F., & Aquino, J. M. (2021). On the performance of distinct
616 electrochemical and solar-based advanced oxidation processes to mineralize the insecticide
617 imidacloprid. *Chemosphere*, *275*, 130010.
618 https://doi.org/10.1016/j.chemosphere.2021.130010.
619 [12] Kowalska, K., Maniakova, G., Carotenuto, M., Sacco, O., Vaiano, V., Lofrano, G., &
620 Rizzo, L. (2020). Removal of carbamazepine, diclofenac and trimethoprim by solar driven
621 advanced oxidation processes in a compound triangular collector based reactor : A

622 comparison between homogeneous and heterogeneous processes. *Chemosphere*, *238*, 124665.
623 https://doi.org/10.1016/j.chemosphere.2019.124665.
624 [13] Rizzo, L., Lofrano, G., Gago, C., Bredneva, T., Iannece, P., Pazos, M., Krasnogorskaya,
625 N., & Carotenuto, M. (2018). Antibiotic contaminated water treated by photo driven advanced
626 oxidation processes : Ultraviolet/H2O2 vs ultraviolet/peracetic acid. *Journal of Cleaner*
627 *Production*, *205*, 67- 75. https://doi.org/10.1016/j.jclepro.2018.09.101.
628 [14] Velo-Gala, I., Pirán-Montaño, J. A., Rivera-Utrilla, J., Sánchez-Polo, M., & Mota, A. J.
629 (2017). Advanced Oxidation Processes based on the use of UVC and simulated solar radiation
630 to remove the antibiotic tinidazole from water. *Chemical Engineering Journal*, *323*, 605- 617.
631 https://doi.org/10.1016/j.cej.2017.04.102.
632 [15] Ilyas, H. & van Hullebush, E.D. (2020). Performance comparison of different types of
633 constructed wetlands for the removal of pharmaceuticals and their transformation products: a
634 review. *Environmental Science and Pollution Research*, 27(14): 1-23.
635 https://doi.org/10.1007/s11356-020-08165-w.
636 [16] Janex-Habibi, M.-L., Huyard, A., Esperanza, M., & Bruchet, A. (2009). Reduction of
637 endocrine disruptor emissions in the environment : The benefit of wastewater treatment.
638 *Water Research*, *43*(6), 1565- 1576. https://doi.org/10.1016/j.watres.2008.12.051.
639 [17] Schilirò, T., Pignata, C., Rovere, R., Fea, E., & Gilli, G. (2009). The endocrine disrupting
640 activity of surface waters and of wastewater treatment plant effluents in relation to
641 chlorination. *Chemosphere*, *75*(3), 335- 340.
642 https://doi.org/10.1016/j.chemosphere.2008.12.028.
643 [18] Adeel, M., Song, X., Wang, Y., Francis, D., & Yang, Y. (2017). Environmental impact of
644 estrogens on human, animal and plant life : A critical review. *Environment International*, *99*,
645 107- 119. https://doi.org/10.1016/j.envint.2016.12.010.

[19] Bolton, J. R., & Stefan, M. I. (2002). Fundamental photochemical approach to the concepts of fluence (UV dose) and electrical energy efficiency in photochemical degradation reactions. *Research on Chemical Intermediates*, *28*(7‐9), 857‐870. https://doi.org/10.1163/15685670260469474.

[20] Sharpless, C. M., & Linden, K. G. (2003). Experimental and Model Comparisons of Low- and Medium-Pressure Hg Lamps for the Direct and H_2O_2 Assisted UV Photodegradation of *N* -Nitrosodimethylamine in Simulated Drinking Water. *Environmental Science & Technology*, *37*(9), 1933‐1940. https://doi.org/10.1021/es025814p.

[21] Shu, Z., Singh, A., Klamerth, N., McPhedran, K., Bolton, J. R., Belosevic, M., & Gamal El-Din, M. (2016). Pilot-scale UV/H2O2 advanced oxidation process for municipal reuse water : Assessing micropollutant degradation and estrogenic impacts on goldfish (Carassius auratus L.). *Water Research*, *101*, 157‐166. https://doi.org/10.1016/j.watres.2016.05.079.

[22] Bolton, J., Bircher, K., Tumas, W., & Tolman, C. (2001). Figures-of merit for the technical development and application of advanced oxidation processes for both electric and solar driven systems. *Pure Appl. Chem.*, *73*(4), 627–637. https://doi.org/10.1351/pac200173040627

[23] Sindelar, H.R., Brown, M.T., & Boyer, T.H. (2014). Evaluating UV/H_2O_2, UV/percarbonate, and UV/perborate for natural organic matter reduction from alternative water sources. *Chemosphere*, *105*, 112-118. https://doi.org/10.1016/j.chemosphere.2013.12.040.

[24] Vishnuganth, M.A., Remya, N., Kumar, M., & Selvaraju, N. (2016). Photocatalytic degradation of carbofuran by TiO_2-coated activated carbon: Model for kinetic, electrical energy per order and economic analysis. *Journal of Environmental Management*, *181*, 201-207. https://doi.org/10.1016/j.jenvman.2016.06.016

670 [25] Andrews, S., Huck, P., Chute, A., Bolton, J., &Anderson, W. (1995). UV oxidation for
671 drinking water – feasibility studies for addressing specific water quality issues. *AWWA*
672 *Annual Conference*, 1881–1898, cited by [23].
673 [26] Hokanson, D. R., Li, K., & Trussell, R. R. (2016). A photolysis coefficient for
674 characterizing the response of aqueous constituents to photolysis. *Frontiers of Environmental*
675 *Science & Engineering*, *10*(3), 428- 437. https://doi.org/10.1007/s11783-015-0780-3.
676 [27] Herrmann, H. (2007). On the photolysis of simple anions and neutral molecules as
677 sources of O^-/OH, SO_x^- and Cl in aqueous solution. *Phys. Chem. Chem. Phys.*, *9*(30),
678 3935- 3964. https://doi.org/10.1039/B618565G.
679 [28] Goldstein, S., Aschengrau, D., Diamant, Y., & Rabani, J. (2007). Photolysis of Aqueous
680 H_2O_2: Quantum Yield and Applications for Polychromatic UV Actinometry in
681 Photoreactors. *Environmental Science & Technology*, *41*(21), 7486- 7490.
682 https://doi.org/10.1021/es071379t.
683 [29] Mark, G., Schuchmann, M. N., Schuchmann, H.-P., & von Sonntag, C. (1990). The
684 photolysis of potassium peroxodisulphate in aqueous solution in the presence of tert-butanol:
685 A simple actinometer for 254 nm radiation. *Journal of Photochemistry and Photobiology A:*
686 *Chemistry*, *55*(2), 157- 168. https://doi.org/10.1016/1010-6030(90)80028-V.
687 [30] Moreira, F. C., Soler, J., Alpendurada, M. F., Boaventura, R. A. R., Brillas, E., & Vilar,
688 V. J. P. (2016). Tertiary treatment of a municipal wastewater toward pharmaceuticals removal
689 by chemical and electrochemical advanced oxidation processes. *Water Research*, *105*,
690 251- 263. https://doi.org/10.1016/j.watres.2016.08.036.
691 [31] Huang, F., Gao, F., Li, C., & Campos, L. C. (2022). Photodegradation of free estrogens
692 driven by UV light: Effects of operation mode and water matrix. *Science of The Total*
693 *Environment*, *835*, 155515. https://doi.org/10.1016/j.scitotenv.2022.155515.

694 [32] Rosenfeldt, E.J. & Linden, K.G. (2004). Degradation of endocrine disrupting chemicals
695 bisphenol A, ethinyl estradiol, and estradiol during UV photolysis and advanced oxidation
696 processes. *Environment Science and technology,* 15;38(20):5476-83.
697 https://doi.org/10.1021/es035413p.
698 [33] Ma, J., Yang, Y., Jiang, X., Xie, Z., Li, X., Chen, C., & Chen, H. (2018). Impacts of
699 inorganic anions and natural organic matter on thermally activated persulfate oxidation of
700 BTEX in water. *Chemosphere*, *190*, 296- 306.
701 https://doi.org/10.1016/j.chemosphere.2017.09.148.
702 [34] Olmez-Hanci, T., Dursun, D., Aydin, E., Arslan-Alaton, I., Girit, B., Mita, L., Diano, N.,
703 Mita, D. G., & Guida, M. (2015). S2O82−/UV-C and H2O2/UV-C treatment of Bisphenol A :
704 Assessment of toxicity, estrogenic activity, degradation products and results in real water.
705 *Chemosphere*, *119*, S115- S123. https://doi.org/10.1016/j.chemosphere.2014.06.020.
706 [35] Wang, J., & Wang, S. (2021). Effect of inorganic anions on the performance of advanced
707 oxidation processes for degradation of organic contaminants. *Chemical Engineering Journal*,
708 *411*, 128392. https://doi.org/10.1016/j.cej.2020.128392.
709 [36] Lutze, H. V., Bircher, S., Rapp, I., Kerlin, N., Bakkour, R., Geisler, M., von Sonntag, C.,
710 & Schmidt, T. C. (2015). Degradation of Chlorotriazine Pesticides by Sulfate Radicals and the
711 Influence of Organic Matter. *Environmental Science & Technology*, *49*(3), 1673- 1680.
712 https://doi.org/10.1021/es503496u.
713 [37] Imai, A., Fukushima, T., Matsushige, K., Kim, Y.-H., & Choi, K. (2002).
714 Characterization of dissolved organic matter in effluents from wastewater treatment plants.
715 *Water Research*, *36*(4), 859- 870. https://doi.org/10.1016/S0043-1354(01)00283-4.
716 [38] Ma, H., Allen, H. E., & Yin, Y. (2001). Characterization of isolated fractions of
717 dissolved organic matter from natural waters and a wastewater effluent. *Water Research*,
718 *35*(4), 985- 996. https://doi.org/10.1016/S0043-1354(00)00350-X.

719 [39] Yu, J., Lv, L., Lan, P., Zhang, S., Pan, B., & Zhang, W. (2012). Effect of effluent organic
720 matter on the adsorption of perfluorinated compounds onto activated carbon. *Journal of*
721 *Hazardous Materials*, *225*‐ *226*, 99‐ 106. https://doi.org/10.1016/j.jhazmat.2012.04.073.
722 [40] Fu, Y., Gao, X., Geng, J., Li, S., Wu, G., & Ren, H. (2019). Degradation of three
723 nonsteroidal anti-inflammatory drugs by UV/persulfate : Degradation mechanisms, efficiency
724 in effluents disposal. *Chemical Engineering Journal*, *356*, 1032‐ 1041.
725 https://doi.org/10.1016/j.cej.2018.08.013.
726 [41] Kwon, M., Kim, S., Yoon, Y., Jung, Y., Hwang, T.-M., Lee, J., & Kang, J.-W. (2015).
727 Comparative evaluation of ibuprofen removal by UV/H2O2 and UV/S2O82− processes for
728 wastewater treatment. *Chemical Engineering Journal*, *269*, 379‐ 390.
729 https://doi.org/10.1016/j.cej.2015.01.125.
730 [42] Dong, S., Zhai, X., Pi, R., Wei, J., Wang, Y., & Sun, X. (2020). Efficient degradation of
731 naproxen by persulfate activated with zero-valent iron : Performance, kinetic and degradation
732 pathways. *Water Science and Technology*, *81*(10), 2078‐ 2091.
733 https://doi.org/10.2166/wst.2020.263.
734 [43] Yu, H., Nie, E., Xu, J., Yan, S., Cooper, W. J., & Song, W. (2013). Degradation of
735 Diclofenac by Advanced Oxidation and Reduction Processes : Kinetic Studies, Degradation
736 Pathways and Toxicity Assessments. *Water Research*, *47*(5), 1909‐ 1918.
737 https://doi.org/10.1016/j.watres.2013.01.016.
738 [44] Mahdi Ahmed, M., Barbati, S., Doumenq, P., & Chiron, S. (2012). Sulfate radical anion
739 oxidation of diclofenac and sulfamethoxazole for water decontamination. *Chemical*
740 *Engineering Journal*, *197*, 440‐ 447. https://doi.org/10.1016/j.cej.2012.05.040.
741 [45] Autin, O., Romelot, C., Rust, L., Hart, J., Jarvis, P., MacAdam, J., Parsons, S. A., &
742 Jefferson, B. (2013). Evaluation of a UV-light emitting diodes unit for the removal of

743 micropollutants in water for low energy advanced oxidation processes. *Chemosphere*, *92*(6),
744 745- 751. https://doi.org/10.1016/j.chemosphere.2013.04.028.
745 [46] Rodríguez-Chueca, J., Ferreira, L. C., Fernandes, J. R., Tavares, P. B., Lucas, M. S., &
746 Peres, J. A. (2015). Photocatalytic discolouration of Reactive Black 5 by UV-A LEDs and
747 solar radiation. *Journal of Environmental Chemical Engineering*, *3*(4), 2948- 2956.
748 https://doi.org/10.1016/j.jece.2015.10.019.
749 [47] Matafonova, G., & Batoev, V. (2018). Recent advances in application of UV light-
750 emitting diodes for degrading organic pollutants in water through advanced oxidation
751 processes : A review. *Water Research*, *132*, 177- 189.
752 https://doi.org/10.1016/j.watres.2017.12.079.
753

Supplementary Materials

Pilot-scale assessment of the viability of UVA radiation for H_2O_2 or $S_2O_8^{2-}$ activation in advanced oxidation processes

Anaëlle Gabet[1,2], Christine de Brauer[1], Gilles Mailhot[2], Marcello Brigante[2], Hélène Métivier[1]

[1] Univ Lyon, INSA Lyon, DEEP, EA7429, 69621 Villeurbanne, France

[2] Université Clermont Auvergne, CNRS, Clermont Auvergne INP, Institut de Chimie de Clermont-Ferrand, F-63000 Clermont-Ferrand, France

*corresponding author: helene.metivier@insa-lyon.fr

Figure SM1. UVA lamp emission spectrum (Philips).

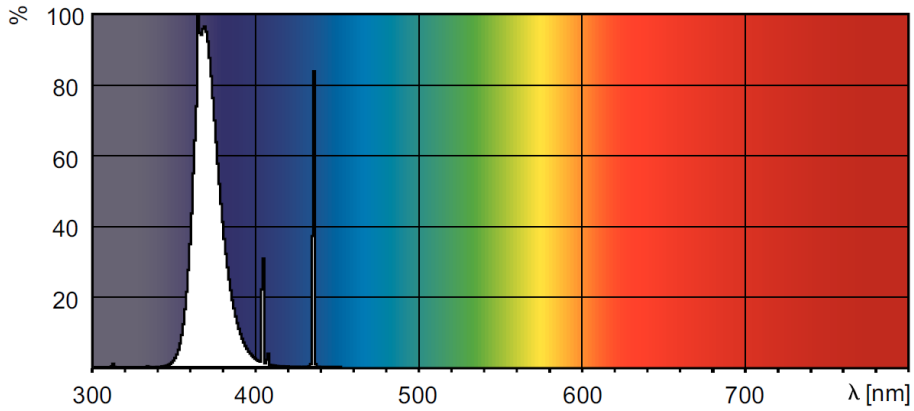

Figure SM2.Examples of typical chromatogram for a) estrogens and b) pharmaceuticals..

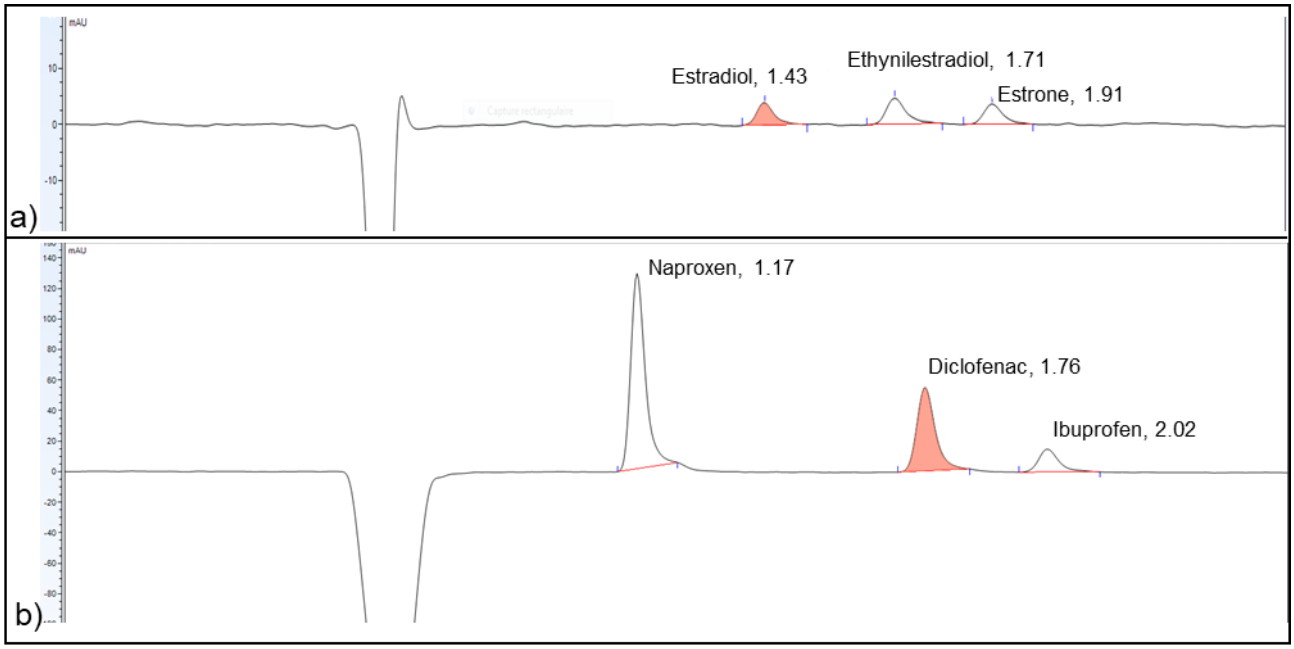

Figure SM3. UVA-based processes for estrogens degradation in drinking water.

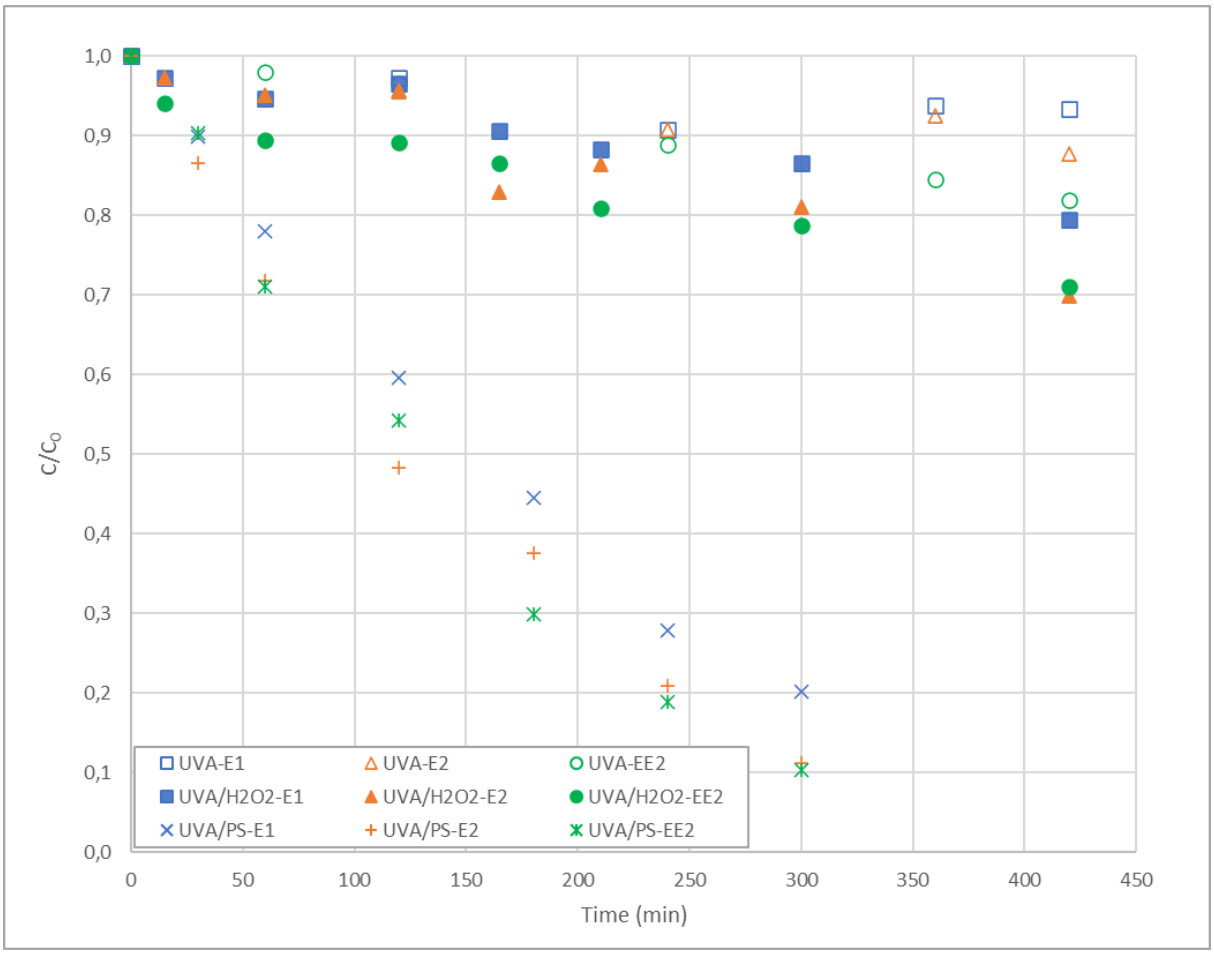

Initial concentration of estrogens: 5 µM each; initial concentration of radical precursor (hydrogen peroxide (H2O2) or persulphate ions (PS)): 1 mM; aqueous matrix is drinking water (Table 2).

Figure SM4. UVC-based processes for estrogens degradation in drinking water.

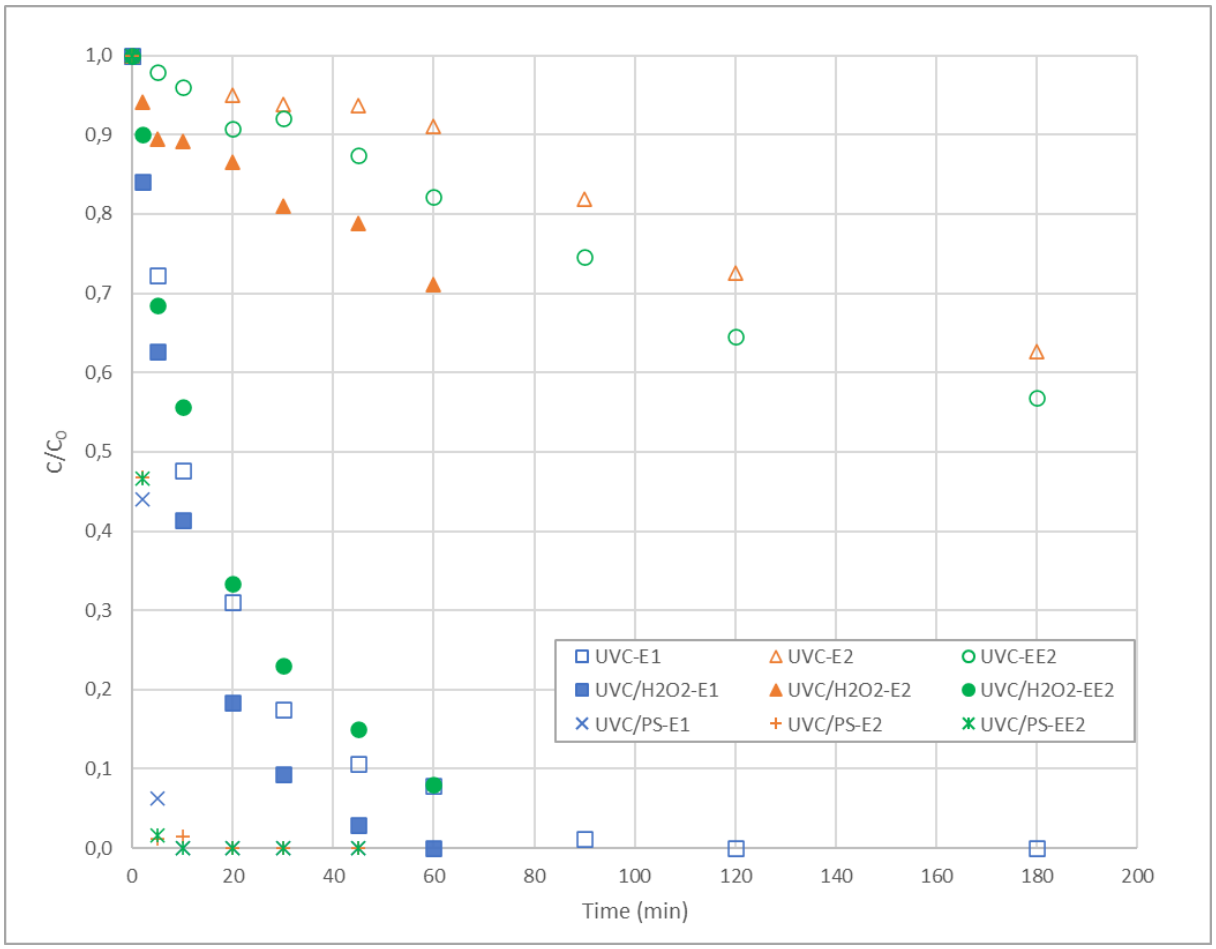

Initial concentration of estrogens: 5 µM each; initial concentration of radical precursor (hydrogen peroxide (H2O2) or persulphate ions (PS)): 1 mM; aqueous matrix is drinking water (Table 2).

Figure SM5. AOPs for estrogens degradation in WWTP effluent.

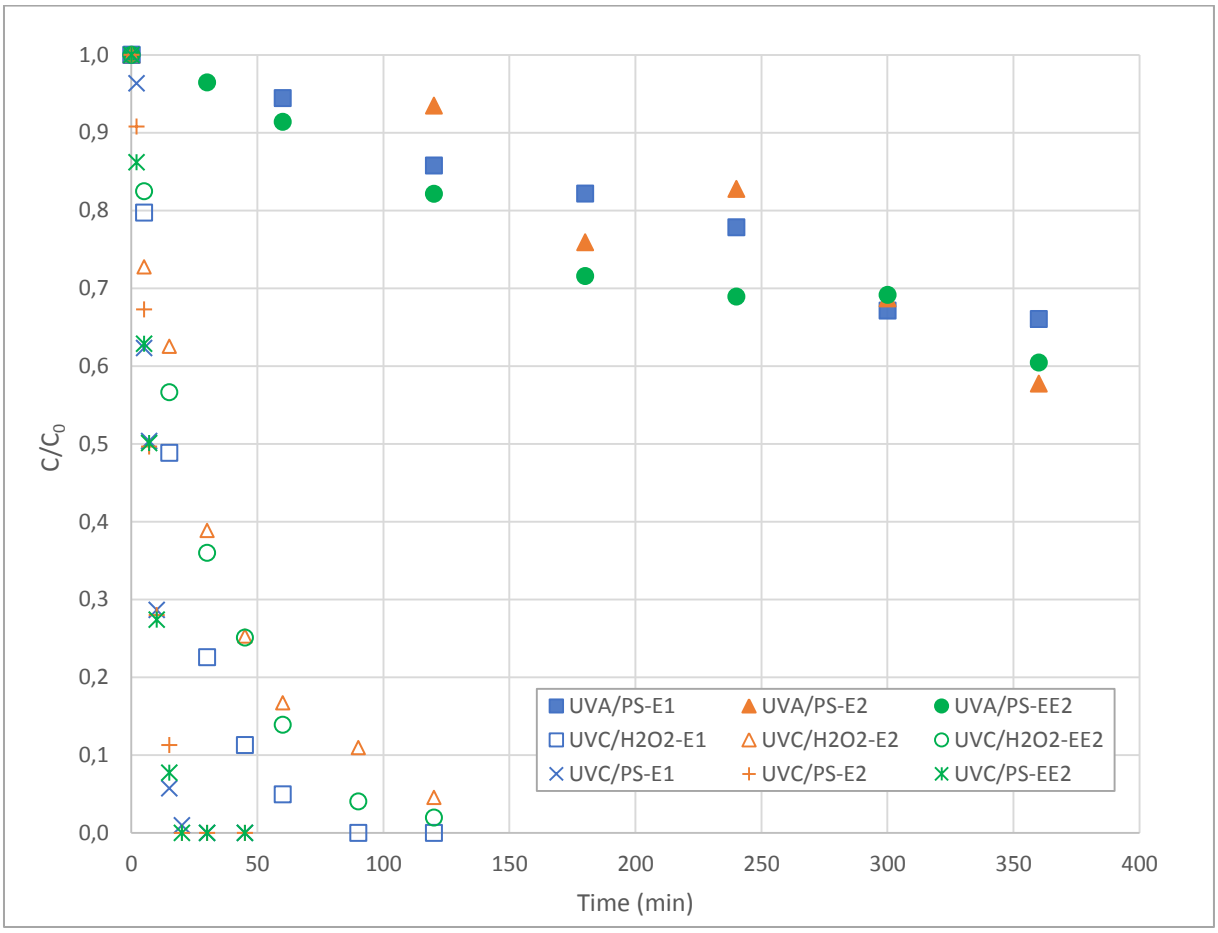

Initial concentration of estrogens: 5 µM each; initial concentration of radical precursor (hydrogen peroxide (H2O2) or persulphate ions (PS)): 1 mM; aqueous matrix is WWTP effluent 1 (Table 2).

Figure SM6. AOPs for pharmaceuticals degradation in WWTP effluent.

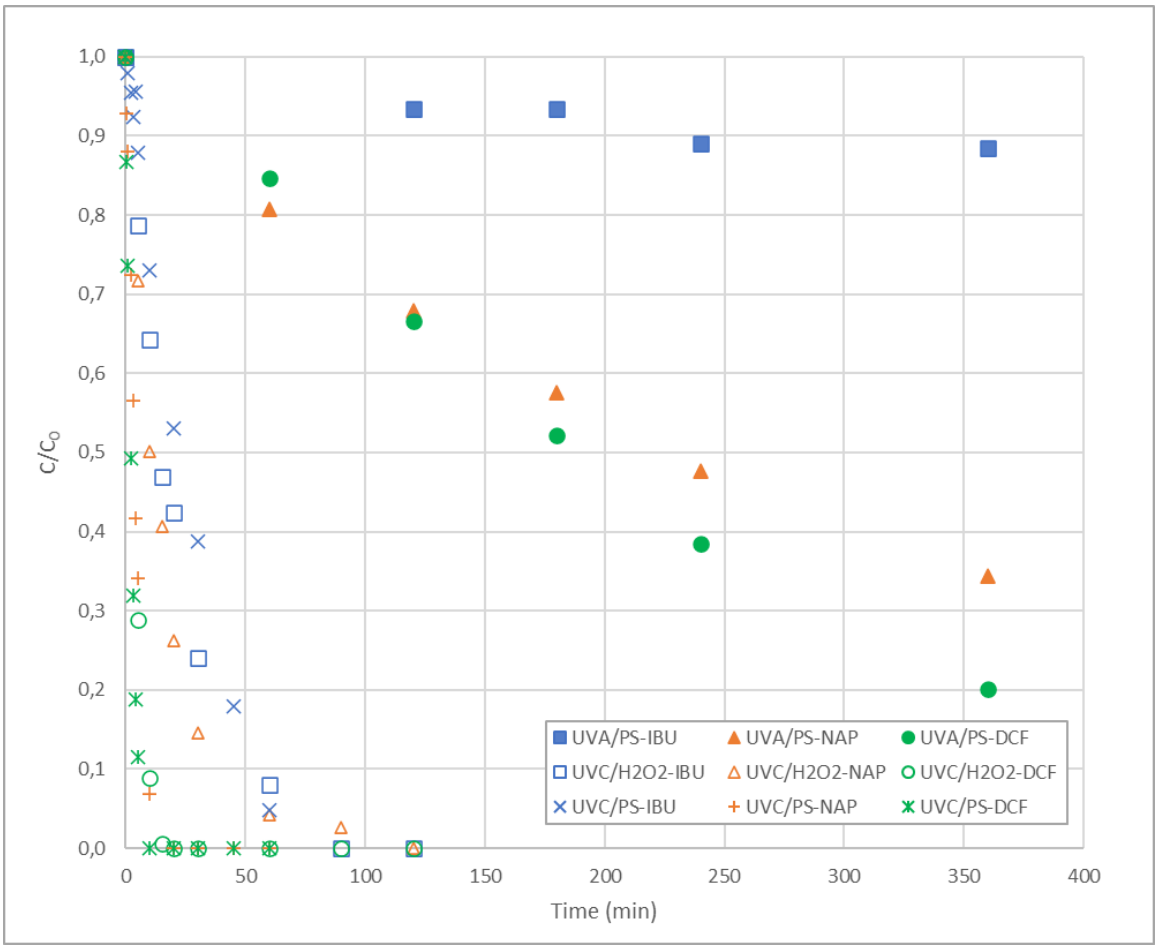

Initial concentration of pharmaceuticals: 5 µM each; initial concentration of radical precursor (hydrogen peroxide (H2O2) or persulphate ions (PS)): 1 mM; aqueous matrix is WWTP effluent 2 (Table 2)

798 *Table SM1. Estimates of E_{EO} for micropollutant reduction by photolysis or different AOPs.*

Matrix	Radiation type	Oxidant precursor	Time (min)	Target molecule	C_i (µM)	C_f (µM)	E_{EO} (kWh m^{-3} $order^{-1}$)
Estrogens							
Drinking water	UVA	None	420	E1	4.09	3.82	424.8
				E2	4.60	4.04	223.5
				EE2	4.38	3.59	145.9
	UVC	None	90	E1	4.21	0.05	2.1
				E2	4.29	3.52	47.1
				EE2	4.49	3.35	31.8
	UVA	H_2O_2	420	E1	4.20	3.34	126.6
				E2	4.50	3.15	81.3
				EE2	4.57	3.24	84.4
		$S_2O_8^{2-}$	240	E1	4.32	0.87	10.3
				E2	4.51	0.51	7.6
				EE2	4.61	0.48	7.3
	UVC	H_2O_2	30	E1	4.72	0.44	1.3
				E2	4.86	1.17	2.2
				EE2	4.75	1.09	2.1
		$S_2O_8^{2-}$	5	E1	3.99	0.25	0.2
				E2	4.26	0.06	0.1
				EE2	5.35	0.09	0.1
WWTP effluent 1	UVA	$S_2O_8^{2}$	360	E1	4.38	2.89	59.8
				E2	4.38	2.79	55.1
				EE2	4.78	2.89	49.4
	UVC	H_2O_2	60	E1	4.75	0.23	2.1
				E2	4.85	0.81	3.5
				EE2	5.07	0.71	3.2
		$S_2O_8^{2-}$	7	E1	4.1	1.89	0.9
				E2	4.34	1.99	0.9
				EE2	4.78	2.14	0.9
Pharmaceuticals							
WWTP effluent 2	UVA	$S_2O_8^{2-}$	360	IBU	5.42	4.79	203.1
				NAP	4.71	1.62	23.3
				DCF	4.34	0.87	15.5
	UVC	H_2O_2	15	IBU	5.70	2.67	2.1
				NAP	5.38	2.18	1.7
				DCF	4.70	0.03	0.3
		$S_2O_8^{2-}$	5	IBU	5.15	4.53	4.0
				NAP	4.03	1.38	0.5
				DCF	4.03	0.46	0.2

799

800

Table SM2. Pseudo-first order degradation constants of E1, E2 and EE2 in the different processes with two different matrices and the degradation rates at 1000 mJ cm^{-2} in WWTP effluent 1.

			Drinking water	WWTP effluent 1	
Radiation type	Oxidant precursor	Estrogen	Rate constants k' (cm^2 mJ^{-1})		Degradation at 1000 mJ cm^{-2} (%)
UVA	$S_2O_8^{2-}$	E1	2.1×10^{-4}	5.2×10^{-5}	5
		E2	2.8×10^{-4}	5.5×10^{-5}	5
		EE2	3.0×10^{-4}	6.3×10^{-5}	6
UVC	H_2O_2	E1	1.7×10^{-3}	1.2×10^{-3}	71
		E2	9.4×10^{-4}	6.6×10^{-4}	48
		EE2	9.5×10^{-4}	8.4×10^{-4}	43
	$S_2O_8^{2-}$	E1	1.1×10^{-2}	2.3×10^{-3}	90
		E2	1.1×10^{-2}	2.3×10^{-3}	90
		EE2	1.1×10^{-2}	2.4×10^{-3}	91

Table SM3. Pseudo-first order degradation constants of IBU, NAP and DCF in the different processes with WWTP effluent 2 as a matrix and the degradation rates at 1000 mJ cm^{-2}.

Radiation type	Oxidant precursor	Pharmaceuticals	Rate constants k' (cm^2 mJ^{-1})	Degradation at 1000 mJ cm^{-2} (%)
UVA	$S_2O_8^{2-}$	IBU	1.7×10^{-5}	2
		NAP	1.3×10^{-4}	13
		DCF	1.8×10^{-4}	17
UVC	H_2O_2	IBU	1.1×10^{-3}	66
		NAP	1.4×10^{-3}	75
		DCF	7.7×10^{-3}	100
	$S_2O_8^{2-}$	IBU	8.7×10^{-4}	58
		NAP	5.1×10^{-3}	99
		DCF	1.0×10^{-2}	100